Wide-band Oscillation Detection Using High-Speed Synchrophasor Measurements Based on a Time-Frequency Method

Yi Zhao¹, Yilu Liu^{1,2}
1. The University of Tennessee, Knoxville
2. Oak Ridge National Laboratory
TN, USA
yzhao77@utk.edu, liu@utk.edu

Abstract— Increasing renewable penetration in interconnected power grids has led to a higher occurrence of low-frequency oscillations (LFOs) and subsynchronous oscillations (SSOs). Ensuring the secure operation of the power grid necessitates effective wide-band oscillation online detection. This study proposes a novel time-frequency technique for the wide-band oscillation detection and modal parameter identification. Firstly, fast Fourier transform (FFT) with an AI-based clustering method is used to calculate the time-frequency spectrum matrix using high-speed phasor measurement unit (PMU) data. This matrix facilitates the accurate estimation of the total number of LFOs and SSOs, along with their start and end times. Additionally, an ARMA-FFT algorithm, considering environmental noise, is proposed for modal parameter estimation, including oscillation frequency, amplitude, phase angle, and damping factor. The accuracy of the proposed method is validated using data from different oscillation events with various ambient noise levels, demonstrating its effectiveness in multimodal analysis and robust resistance to noise.

Index Terms—wide-band oscillation, high-speed phasor measurement unit (PMU), subsynchronous oscillation (SSO), time-frequency analysis

I. INTRODUCTION

The rapid integration of renewable power sources, such as wind and photovoltaic energy, into power systems has led to an increased occurrence of oscillation events in daily operations. Real-world incidents, including subsynchronous oscillations (SSOs), natural low frequency oscillations (LFOs) and forced oscillations, have been observed in various power systems, including the Electric Reliability Council of Texas (ERCOT) power system [1], Great Britain power system [2], and Continental European power system [3]. These incidents jeopardize the secure operation of the system, with the potential for severe stability accidents and equipment damage [4]-[6]. Despite substantial efforts in the detection, modeling, and control of either SSOs or LFOs [7], [8], there has been limited research on the real-time monitoring and detection of wideband oscillations, which include both SSOs and LFOs.

This work was supported by National Science Foundation under the Award Number 1941101 and DOE AGM project. This work also made use of Engineering Research Center Shared Facilities supported by the Engineering Research Center Program of the National Science Foundation and DOE under NSF Award Number EEC-1041877 and the CURENT Industry Partnership Program.

Phasor Measurement Units (PMUs) and Wide Area Measurement Systems (WAMS) has played an important role in detecting and controlling LFOs [9]. Recent research has explored the use of synchrophasors to capture SSO dynamics through various methods, including time domain [10], frequency domain [11], time-frequency domain [12], and artificial intelligence (AI)-based approaches [13]. However, the current design of PMUs, which is tailored for fundamental phasors at frequencies of 50/60 Hz or lower, introduces challenges in accurately capturing SSO dynamics due to signal aliasing and low reporting rates [14]. Moreover, real-world PMU measurements often include environmental noise, and aforementioned analysis methods have limitations in providing high mode resolution and anti-noise capabilities, which are essential for detecting both LFO and SSOs.

To overcome these challenges, a distribution-level PMU, named universal grid analyzer (UGA), has been developed at the University of Tennessee, Knoxville. UGA is capable of streaming real-time measurements with a sampling rate of up to 1440Hz [15]. Utilizing these advanced high-speed UGA measurements, this paper proposes a rapid wide-band oscillation detection algorithm that employs FFT and an AI-based clustering method. This method enables the accurate capture of the start and end times of all oscillation modes based on a time-frequency spectrum matrix. Furthermore, a real-time wide-band oscillation modal analysis method, which combined the Auto Regressive Moving Average (ARMA) and FFT method, is proposed for modal parameter identification of each detected mode with a strong anti-noise ability.

Compared to existing oscillation identification method, the proposed method in this paper has several notable advantages:

1) It does not require any prior knowledge of oscillations or power system models. 2) It can detect all oscillation modes across a wide frequency band using high-sampling-rate PMU data and accurately estimate their modal characteristics. 3) It exhibits strong anti-noise capability under various operating scenarios, making it highly suitable for different types of oscillation detection and mode analysis in real-time.

The remainder of this paper is organized as follows. Section II describes the algorithms used for wide-band oscillation detection and modal parameter identification. The procedure of the proposed methods is summarized in Section III. Section IV presents the performance evaluation of the proposed method using various testing signals and field data in the Kaua'i power system. Section V gives the conclusion of the paper.

II. WIDE-BAND OSCILLATION DETECTION METHOLOGY

A. Problem Statement

Considering that both LFOs and SSOs can be triggered by disturbances in the power grid, the bus frequency measured by UGAs at different locations can always provide observations of all oscillation modes. Assume y(t) is one UGA frequency data containing M oscillation modes, which can be expressed as the following equation (1).

$$y(t) = \sum_{m=1}^{M} A_m e^{-i\zeta_m 2\pi f_m t} \cos(2\pi f_m t + \theta_m)$$
 (1)

The problems are to determine the oscillation mode number M, and to identify the frequency f_m , corresponding amplitude A_m , phase angle θ_m , and damping factor ζ_m for each mode.

B. Total Oscillation Mode Number Estimation

This paper proposes an iterative K-means combined with FFT method to detect the total number of oscillation modes during disturbances, taking into account spectrum leakage and environmental noise impact. When oscillations are excited by external disturbances, the magnitude in the frequency domain at the dominant oscillation frequency significantly exceeds that of normal ambient data. Through statistical analysis of the ambient noise spectrum magnitude using FFT, the maximum FFT magnitude within a broad frequency range is identified and labeled as α_{noise} . Considering spectrum leakage from the FFT, the frequencies whose FFT spectrum magnitudes are larger than α_{noise} and satisfy (2) are selected as candidate dominant oscillation modes using a 50-s sliding window UGA data with 100ms refresh time step. The sliding window is set to 50s with the following considerations: 1) At least 4~5 cycles of oscillation data are required to accurately calculate modal characteristics, such as the damping ratio and magnitude; 2) The LFOs is usually between 0.1Hz to 2Hz, implying that one oscillation cycle can last approximately 10 seconds. Taking these factors into account, a 50-s window length is chosen for the analysis

$$\begin{cases} |\Phi(\omega_{k})| > \alpha_{ns} \\ (|\Phi(\omega_{k})| - |\Phi(\omega_{k-1})|)/(\omega_{k} - \omega_{k-1}) > 0 \\ (|\Phi(\omega_{k+1})| - |\Phi(\omega_{k})|)/(\omega_{k+1} - \omega_{k}) < 0 \end{cases}$$
 (2)

For each 50-s sliding window of data, the iterative K-means method is applied to the spectrum $\{|\Phi(\omega_k)|\}$ of the candidate modes $\{\omega_k\}$ to further mitigate spectrum leakage impact from FFT and to identify the dominant modes. In each iteration, the K-means with 2 centroids will be conducted on $\{\Phi(\omega_k)\}$ to get the cluster $\{\Phi(\omega_{k1})\}$ with the larger centroid. This cluster is selected to count the total number of modes M_{lk} within $\{\omega_{k1}\}$ that satisfies $(\omega_{k1}(j+1)-\omega_{k1}(j))/2\pi>0.1$ Hz. This process of K-means clustering with 2 centroids is iteratively conducted till $M_{lk}=\operatorname{card}(\{\omega_{k1}\})-1$. All the selected modes in $\{\omega_{k1}\}$ from the final iteration are the dominate oscillation modes

obtained in each 50-s sliding window of data. Through this iterative process, the impact of spectrum leakage can be effectively eliminated.

By applying a 50-s sliding window with a 100ms refresh time step to y(t), the spectrum magnitude curve $|\Phi_m(t)|$ at the dominant mode f_m (i.e., $2\pi\omega_m$) with respect to time t can be obtained and stored in a time-frequency matrix M_m . A new row will be added to M_m with each 100ms increment in time. To mitigate the random noise and bad data impacts, only those modes that last over 5 seconds (i.e., more than 50 consecutive non-zero rows of M_m) will be identified as the dominant modes and signifies the detection of an oscillation event. This detection will trigger two key processes: estimating the duration of the oscillation event and conducting a modal parameter estimation.

C. Oscillation Event Duration Estimation

An event data with multiple modes is shown as Fig.1. For this analysis, it is assumed that, i.e., $\zeta_m > 0, m = 1, \cdots M$. Based on the curve $|\Phi_m(t)|$ of the dominant mode f_m , window C in Fig.1, which has the sharpest slope change represents the start time t_{ms} of the event. The end time t_{me} of the event, represented by window D, is identified as the point when $|\Phi_m(t)|$ returns to zero.

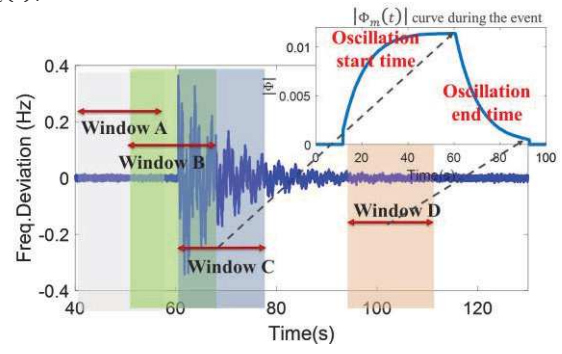


Figure 1. Spectrum magnitude curve $|\Phi_m(t)|$ at dominant mode f_m during an oscillation event

D. Modal Parameter Identification with Time-Frequency Method

After getting the start time t_{ms} , the UGA data from the interval $[t_{ms}, t_{ms} + 50]$ is collected for modal parameter estimation. In this phase, the frequency f_m , amplitude A_m , phase angle θ_m , and damping factor ζ_m of mode m can be calculated using an auto regressive moving average (ARMA)-FFT method. The ARMA model for y(t) can be expressed as

$$y(t) = \sum_{i=1}^{N_{ar}} \varphi_i y(t-j) - \sum_{i=1}^{N_{ma}} \tau_i e(t-j)$$
 (3)

where φ_j is the coefficients of AR part to capture the oscillation frequency and damping factor, while τ_j is the coefficients of MA part, which represents the ambient noise caused by the load variations in the daily operation of a power system [16]. N_{ar} and N_{ma} are the orders of AR and MA parameters, which can be determined using the Akaike Information Criterion (AIC) and Bayesian Information Criterion (BIC).

Based on the autocorrelation function of y(t), φ_j is estimated through Yule-Walker equation. The frequency and damping factor of oscillation mode j can be obtained from (4)

$$\begin{cases}
\sigma^{N_{ar}} + \sum_{j=1}^{N_{ar}} \varphi_j \sigma^{N_{ar}-j} = 0 \\
f_j = \frac{f_s}{2\pi} \left| \ln(\sigma_j) \right|, \quad \zeta_j = \frac{-Re\{\ln(\sigma_j)\}}{|\ln(\sigma_j)|}
\end{cases} \tag{4}$$

where σ_j is the *j*-th root of the polynomial in equation (4) and f_s is the sampling rate of y(t).

By comparing the mode frequencies f_j as obtained from equation (4), with f_m , as determined in Section II.B, the mode with the closest frequency to f_m is selected. This frequency is then designated as the estimated frequency \hat{f}_m , and the corresponding damping factor $\hat{\zeta}_m$ is simultaneously obtained.

To estimate the amplitude A_m and phase angle θ_m , two standard 50-s synthetic ideal oscillation signals are generated with an amplitude of 1 p.u. as follows:

$$\begin{cases} S_{m1}(t) = e^{-i\hat{\zeta}_m 2\pi \hat{f}_m t} \cos(2\pi \hat{f}_m t) \\ S_{m2}(t) = \cos(2\pi \hat{f}_m t) \end{cases}$$
 (5)

The gain introduced by the damping factor is calculated using the following equation:

$$G_{ms} = \sum_{t=0}^{50} |S_{m1}(t)| / \sum_{t=0}^{50} |S_{m2}(t)|$$
 (6)

The amplitude A_m and phase angle θ_m can be estimated based on the spectrum magnitude $|\Phi_m(t)|$ as following

$$\hat{A}_m = |\Phi_m(t_{ms})| G_{ms} \tag{7}$$

$$\hat{\theta}_m = \angle \Phi_m(t_{ms}) \tag{8}$$

III. PROCEDURE OF WIDE-BAND OSCILLATION DETECTION

According to Section II, the procedure for online wide-band oscillation detection and modal parameter estimation in Fig. 2 can be summarized as follows:

- Step 0: Collect UGA data at time t_k with a 50-s sliding window.
- Step 1: Preprocess data: identify and handle random bad data and long-term data loss. Replace random bad data using interpolation techniques. If data loss lasts over 1 second, discard the data and replace it all with 0.
- Step 2: Use iterative K-means combined with FFT method to estimate the total oscillation mode numbers. Obtain spectrum magnitude $|\Phi_m(t_k)|$ for dominate mode f_m at t_k , and save in time-frequency matrix M_m for mode f_m .
- Step 3: Get the consecutive non-zero rows of M_m and save as $M'_m(t_k)$ at t_k . Check if the number of consecutive non-zero rows of M_m is over 50.
- Step 4: Estimate the oscillation start time t_{ms} based on $f_m(t)$ and $|\Phi_m(t)|$.
- Step 5: Calculate modal parameters with ARMA-FFT method.
- Step 6: Check if the size of $M'_m(t_{k-1})$ is equal to the size of $M'_m(t_k)$ and calculate the oscillation end time t_{me} .

Step 7:
$$k = k + 1$$
, $t_k = t_0 + k \cdot T_{ms}$ with $T_{ms} = 100ms$.

Step 8: repeat Step 0-5 until t_k reach the end of the UGA data length or the end of the simulation.

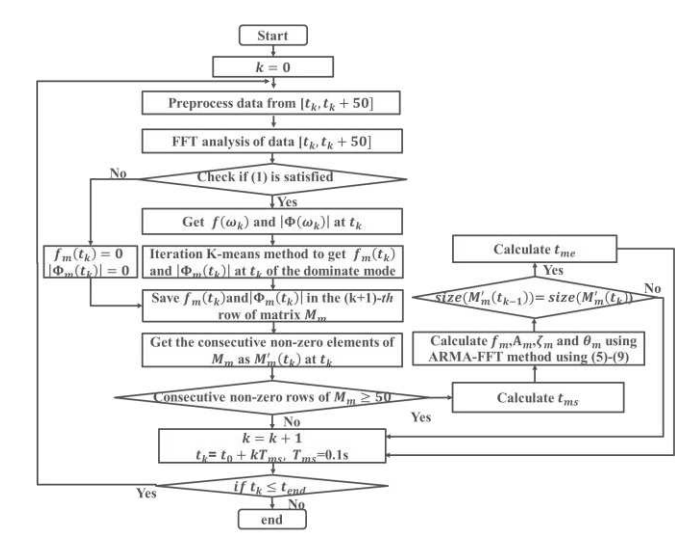


Figure 2. Flow chart of the proposed wide-band oscillation detection and modal parameter estimation method

IV. STUDY CASES

In this section, the proposed technique is validated using a range of data sets, including both simulated wide-band oscillation events, and real field oscillation event data. Additionally, the impact of various environmental noise levels on the performance of the proposed method is also examined. To save space, the data preprocessing process will not be discussed in these study cases.

A. Oscillation Detection and Modal Parameter Estimation of Ideal Synthetic Signal

To validate the efficiency of the proposed method, synthetic data comprising three distinct oscillation events, including both LFOs and SSOs, are generated with a sampling rate of 200Hz. The total duration of the data is set at 900 s. The start times for the events are as follows: Event 1 at 60.5 seconds, Event 2 at 450.3 seconds, and Event 3 at 737.1 seconds. In Event 1, the two LFOs at 0.3Hz and 12Hz exhibit the highest amplitudes and energy, followed by two SSOs at 30Hz and 24.5Hz with lower amplitudes and energy. In Event 2, two SSOs at 13Hz and 37Hz show higher energy levels, alongside an LFO at 0.75Hz with a smaller amplitude. In Event 3, all the LFOs and SSOs display similar energy levels. The detailed modal characteristics of the LFOs and SSOs for each event are presented as actual values in Table I. Notably, the characteristics of the oscillation modes vary over time across these events, offering valuable insights for assessing the effectiveness of the proposed technology in online applications, particularly under varying power grid operating conditions.

The FFT analysis results of the 900-s synthetic event data are displayed in Fig.3, which illustrates the wide distribution of the dominant oscillation modes. However, FFT analysis primarily provides an overview of the signal's overall frequency characteristics, and this method has limitations in capturing the temporal changes of time-varying oscillation signals.

By utilizing the proposed method in this paper, the estimated modal parameters for each oscillation mode during the three events are shown in Table I. Since this event data is an ideal signal without noise, α_{ns} in equation (2) is set to 0.0001.

TABLE I MODAL PARAMETER ESTIMATION RESULTS OF IDEAL SYNTHETIC SIGNAL

Event	Freq. (Hz)			Amp. (Hz)			Phase (°)			Damping factor (%)		
	Ture value	Estimated value	Error	Ture value	Estimated value	Error	Ture value	Estimated value	Error	Ture value	Estimated value	Error
	30	30.0000	0.0000	0.06	0.0594	0.0006	90	89.73	0.27	0.053	0.053	0
Event	24.5	24.5000	0.0000	0.08	0.0798	0.0002	36	35.75	0.25	0.065	0.065	0
1	1.2	1.1998	0.0002	0.15	0.1487	0.0013	18	17.01	0.99	1.320	1.330	1e-02
	0.3	0.3000	0.0000	0.16	0.1586	0.0014	0	-1.16	1.16	5.300	5.300	0
Event	37	37.0000	0.0000	0.15	0.1500	0.0000	22	22.39	0.39	0.043	0.043	0
	13	12.9996	0.0004	0.20	0.1989	0.0011	15	14.95	0.05	0.122	0.118	4e-03
2	0.75	0.7500	0.0000	0.05	0.0482	0.0018	30	29.71	0.29	2.120	2.120	0
Г (55	55.0000	0.0000	0.07	0.0683	0.0017	15	14.89	0.11	0.0289	0.0288	1e-04
Event	45	44.9981	0.0019	0.06	0.0600	0.0000	30	30.03	0.03	0.035	0.035	0
3	5.5	5.5000	0.0000	0.06	0.0600	0.0000	20	19.93	0.07	0.289	0.289	0

The results in Table I indicate that the maximum estimated error in oscillation frequency is less than 0.0002 Hz, the estimated phase angle error is less than 1.16 degrees, the estimated oscillation amplitude error is below 2 mHz, and the estimated damping factor error is less than 0.01%. These results demonstrate that the proposed method can accurately capture both the LFO and SSO mode characteristics with high precision.

The estimated start times for the three events are listed in Table II according to the proposed method. The estimated start times precisely match the actual start times of each event, demonstrating the accurate oscillation detection through the proposed method.

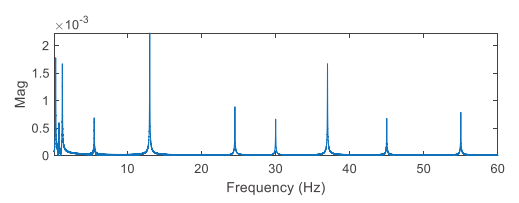


Figure 3. FFT magnitude of ideal synthetic signal

TABLE II. START TIME ESTIMATION RESULTS

Event	Start time (s)							
Event	Ture value	Estimated value						
Event 1	60.5	60.5						
Event 2	450.3	450.3						
Event 3	737.1	737.1						

B. Oscillation Detection and Modal Parameter Identification under Different Noise Evels

Four different ambient noises e_n are added to the synthetic data in Section IV.A respectively. The signal-to-noise (SNR) with the maximum and minimum frequency deviation of the three noises are calculated according to equation (9) and listed in Table III.

$$SNR_f = 20\log(1/(std(e_n) * f_n)) \tag{9}$$

where f_n is set to be 60Hz in this study.

Given that the estimation of the oscillation mode with smaller amplitude is more susceptible to the noise, the 0.75 Hz mode in Event 2 and the 45 Hz mode in Event 3, both characterized by smaller amplitudes, are studied in detail. Fig.4 (a) and (b) show the spectrum magnitude $|\Phi_m(t)|$ for the 0.75Hz mode and the 45 Hz mode, respectively. From the plots, it can be clearly seen that the curves of $|\Phi_m(t)|$ become more fluctuated with the increase of noise level. Even with noise

reaching a maximum amplitude of 40 mHz (e.g., Noise 4 with 77.2 dB), close to the amplitude of the 0.75Hz and 45Hz oscillation mode, the curves still accurately identify the start time of the events at the point with the sharpest slope change. The oscillation start times are precisely estimated at 450.3s and 737.1s across the four different noise levels.

TABLE III. DIFFENT NOISE LEVEL INFORMATION

Noise	SNR	Max (mHz)	Min (mHz)
1	82.5	20.4	-22.8
2	79.65	30.8	-25.4
3	77.76	35.2	-33.7
4	77.24	39.2	-38.9

Table IV lists all the estimated modal parameters for each mode. Compared to the true values, the estimated frequency error is below 0.001Hz, the estimated amplitude error is less than 3mHz, the estimated phase angle error is less than 2.4°, and the estimated damping factor error is less than 0.1%. These testing results proves the significant anti-noise capability of the proposed method in modal characteristics estimation of both LFO and SSO and the accurate detection of the oscillation events.

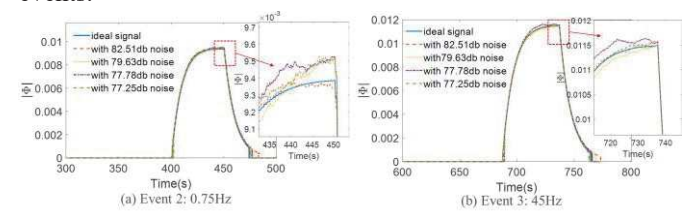


Figure 4. Spectrum magnitude $|\Phi_m(t)|$ of 0.75Hz and 45Hz mode

C. Validation Using Field PMU data

In this section, UGA field data collected from 3 a.m. to 4 a.m. UTC on March 30, 2022, in the Kaua'i power system, is utilized to further validate the performance of the proposed approaches. During this period, the ambient noise level was 77.41 dB. A 20Hz SSO events occurred at 95s as shown in Fig.5, and lasted for several hours due to a nearly 0 damping factor. Both the environmental noise and the bad data was included in the field event data as shown in Fig.5. Utilizing our proposed method, the 20Hz oscillation was successfully detected, with its spectrum magnitude $|\Phi_m(t)|$ depicted in Fig. 6. Differing from the curves in Fig.1 and Fig. 4, $|\Phi_m(t)|$ for this undamped SSO mode in Fig.6 continuously grew to a relatively stable value, rather than returning to zero. The start time of the event was accurately identified at 95s that with the sharpest slope change as described in Section II.C.

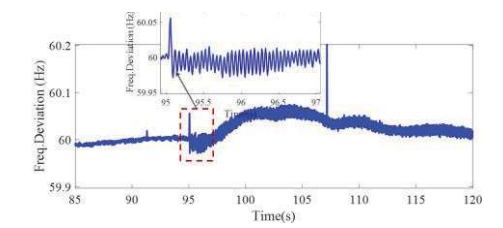


Figure 5. Field data of the 20Hz oscillation event in Kaua'i power system

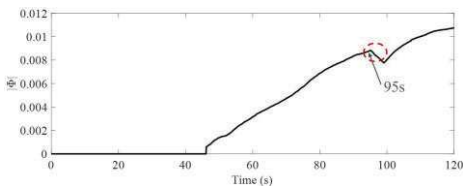


Figure 6. Spectrum magnitude $|\Phi_m(t)|$ of 20Hz mode

Due to the absence of ground truth in the field data, the estimated modal parameters obtained from our proposed method are compared with the results from Prony analysis to evaluate the algorithm's effectiveness. The estimated modal parameters for the 20Hz mode, alongside the Prony analysis results, are presented in Table V. This comparison reveals that the results are almost consistent with each other, further validating the efficacy of our proposed methods.

TABLE V. ESTIMATED MODAL PARAMETERS FOR THE 20HZ MODE

Method	Freq. (Hz)	Amp. (Hz)	Phase (°)	Damping factor (%)	
Proposed method	19.995	0.0167	179.25	0.002	
Prony	20.005	0.0158	173.05	0.111	

V. CONCLUSION

This paper proposes an innovative time-frequency wide-band oscillation detection method capable of detecting all the LFOs and SSOs using real-time high-sampling-rate PMU data. This method can automatically capture the total number of oscillation modes during different events, without relying on any prior information. More importantly, by utilizing testing signals with various levels of ambient noise and field data from the Kaua'i power system, the approach accurately captures event start times and estimates oscillation modal parameters with high accuracy. Given its high precision and strong antinoise capability, this method is well-suited for online applications in the real-time monitoring and analysis of both LFOs and SSOs in power systems.

REFERENCES

 Y. Cheng, M. Podlaski, J. Schmall, S. -H. F. Huang and M. Khan, "ERCOT PSCAD model review platform development and performance

- comparison with PSS/e model," in 2020 IEEE Power & Energy Society General Meeting (PESGM), pp. 1-5
- [2] Y. Zhao, Y. Dong, L. Zhu, K. Sun, K, Alshuaibi, C. Zhang, et al., "Coordinated control of natural and sub-synchronous oscillations via HVDC links in Great Britain power system," in 2022 IEEE/PES Transmission and Distribution Conference and Exposition (T&D), pp. 1-5
- [3] ENTSO-e. (2018, Mar.). Oscillation event 03.12.2017. [Online]. Available: https://eepublicdownloads.entsoe.eu/clean-documents/SOC%20documents/Regional_Groups_Continental_Europe/OSCILLATION_REPORT_SPD.pdf.
- [4] L. Zhu, W. Yu, Z. Jiang, C. Zhang, Y. Zhao, J. Dong, et al., "A comprehensive method to mitigate forced oscillations in large interconnected power grids," *IEEE Access*, vol. 9, pp. 22503-22515, 2021
- [5] M. Wu, L. Xie, L. Cheng, R. Sun, "A study on the impact of wind farm spatial distribution on power system sub-synchronous oscillations," *IEEE Trans. Power System*, vol. 31, no. 3, pp. 2154-2162, May 2016.
- [6] Y. Zhao, L. Zhu, H. Xiao, Y. Liu, E. Farantatos, M. Patel, A. Darvishi and B. Fardanesh, "An adaptive wide-area damping controller via facts for the New York State Grid using a measurement-driven model," in 2019 IEEE Power & Energy Society General Meeting (PESGM), pp. 1-5
- [7] Y. Cheng, L. Fan, J. Rose, S.H. Huangg, J. Schmall, X. Wang, et al., "Real-world subsynchronous oscillation events in power grids with high penetrations of inverter-based resources," *IEEE Trans. Power System*, vol. 38, no. 1, pp. 316-330, Jan. 2023,
- [8] R. Xie, I. Kamwa and C. Y. Chung, "A novel wide-area control strategy for damping of critical frequency oscillations via modulation of active power injections," *IEEE Trans. Power Systems*, vol. 36, no. 1, pp. 485-494, Jan. 2021.
- [9] A. Liccardo, S. Tessitore, F. Bonavolontà, S. Cristiano, L.P.D. Noia, G.M. Giannuzzi, et al., "Detection and analysis of inter-area oscillations through a dynamic-order DMD approach," *IEEE Trans. Instrumentation* and Measurement, vol. 71, pp. 1-14, Jul. 2022.
- [10] C.Wang, C. Liu, J. Yu, and S. Xu, "Research on sub-synchronous oscillation characteristics between PMSG-based wind farms and weak AC grids based on prony method," in *Proc. IEEE 3rd Conf. Energy Internet EnergySyst. Integr. (E12)*, Nov. 2019, pp. 2781-2786.
- [11] F. Zhang, L. Cheng, W. Gao and R. Huang, "Synchrophasors-based identification for subsynchronous oscillations in power systems," *IEEE Trans. Smart Grid*, vol. 10, no. 2, pp. 2224-2233, March 2019.
- [12] E. Sezgin and Ö. Salor, "Analysis of power system harmonic subgroups of the electric arc furnace currents based on a hybrid time-frequency analysis method," *IEEE Trans. Ind. Appl.*, vol. 55, no. 4, pp. 4398–4406, Jul./Aug. 2019.
- [13] H. Liu, Y. Qi, J. Zhao and T. Bi, "Data-Driven subsynchronous oscillation identification using field synchrophasor measurements," *IEEE Trans. Power Delivery.*, vol. 37, no. 1, pp. 165-175, Feb. 2022
- [14] T. Rauhala, A. Gole and P. Järventausta, "Detection of subsynchronous torsional oscillation frequencies using phasor measurement," *Power Delivery*, vol. 31, no. 1, pp. 11–19, Feb.2016.
- [15] H. Yin, W. Yao, L. Zhan, W. Yu, J. Zhao, Y. Liu, "Low cost, flexible, and distribution level universal grid analyser platform: designs and implementations," *IET Generation, Transmission & Distribution*, vol. 14, no. 19, pp. 3945 3952, Oct.2020.
- [16] W. Qiu, Y. Dong, L. Zhu, S.You, Q. Tang, J. Duan, et al., "Ambient-based oscillation mode analysis via dynamic ensemble ITD and ARMA model for converter-based FFR application," in 2020 IEEE 3rd Student Conference on Electrical Machines and Systems (SCEMS), pp. 718-723.

TABLE IV. MODAL PARAMETER ESTIMATION RESULTS UNDER DIFFENT NOISE LEVELS

Mode	Noise level	Freq. (Hz)			Mag. (Hz)			Phase (°)			Damping factor (%)		
		Ture value	Estimated value	Error	Ture value	Estimated value	Error	Ture value	Estimated value	Error	Ture value	Estimated value	Error
0.75Hz in Event 2	82.50	0.75	0.7503	3e-4	0.0500	0.0492	8e-4	30.00	29.23	0.77	2.1200	2.24	1e-1
	79.65	0.75	0.7492	8e-4	0.0500	0.0472	3e-3	30.00	32.25	2.25	2.1200	2.14	2e-2
	77.76	0.75	0.7501	1e-4	0.0500	0.0520	2e-3	30.00	28.91	1.09	2.1200	2.45	3e-1
	77.24	0.75	0.7506	6e-4	0.0500	0.0488	1e-3	30.00	27.85	2.15	2.1200	2.20	8e-2
45Hz in event 3	82.50	45.00	45.0000	2e-5	0.0600	0.0601	6e-5	30.00	30.03	0.03	0.0354	0.0349	5e-4
	79.65	45.00	45.0005	5e-4	0.0600	0.0606	6e-4	30.00	30.21	0.21	0.0354	0.0351	3e-4
	77.76	45.00	45.0007	7e-4	0.0600	0.0589	1e-3	30.00	30.55	0.55	0.0354	0.0358	4e-4
	77.24	45.00	45.0010	1e-3	0.0600	0.0567	3e-3	30.00	29.44	0.56	0.0354	0.0342	1e-3